Supporting information for

ORIGINAL ARTICLE

Chlorella sp.-ameliorated undesirable microenvironment promotes diabetic wound healing

Hangyi Wu[a], Pei Yang[a], Aiqin Li[a], Xin Jin[a,b], Zhenhai Zhang[c,d,*], HuiXia Lv[a,*]

[a]*Department of Pharmaceutics, China Pharmaceutical University, Nanjing 211198, China*

[b]*The Affiliated Suqian First People's Hospital of Nanjing Medical University, Suqian 223800, China*

[c]*Jiangsu Province Academy of Traditional Chinese Medicine, Nanjing 210023, China*

[d]*Affiliated Hospital of Integrated Traditional Chinese and Western Medicine, Nanjing University of Chinese Medicine, Nanjing 210028, China*

Received 8 February 2022; received in revised form 29 April 2022; accepted 12 May 2022

*Corresponding authors. Tel./fax: +86 13912965842 (Huixia Lv); +86 18913823932 (Zhenhai Zhang).

E-mail addresses: Lvhuixia@163.com (Huixia Lv), david23932@163.com (Zhenhai Zhang).

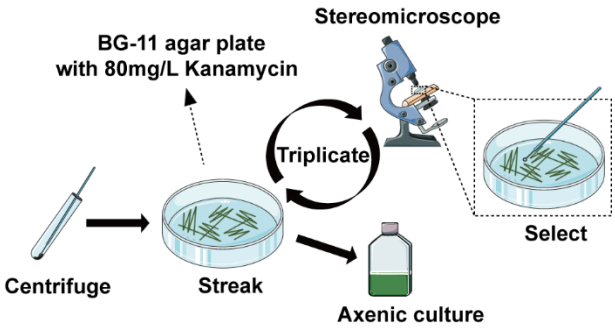

Figure S1 Schematic diagram of Chlorella axenic culture.

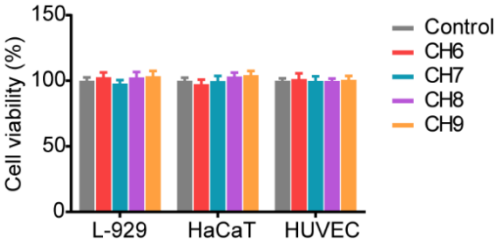

Figure S2 Cytotoxicity of Chlorella hydrogels on L-929, HaCaT and HUVEC cells for 24 h, dark. Data are presented as mean ± SD (*n* = 6).

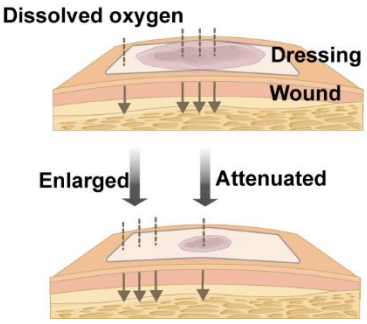

Figure S3 Schematic diagram of dissolved oxygen delivery from hydrogels to the wound area.

Figure S4 Light intensity attenuation by Chlorella hydrogels, left to right: CH6, CH7, CH8 and CH9.

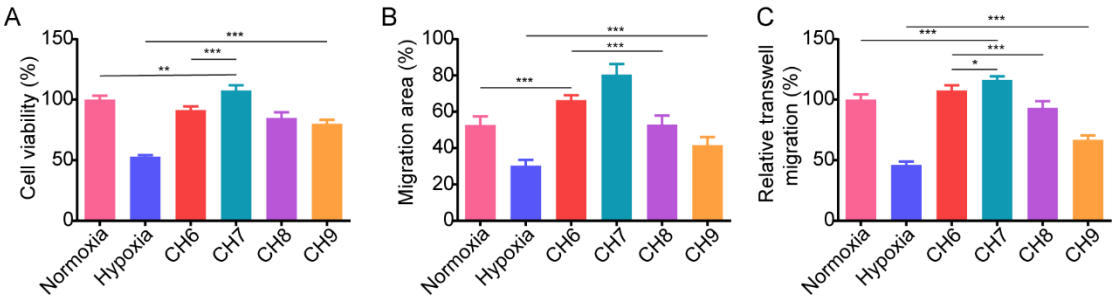

Figure S5 Quantitative analysis of (A) L-929 cell proliferation, (B) HaCaT migration and (C) transwell migration of HUVEC with Chlorella hydrogels in hypoxia condition by ImageJ software, 37 °C, 800 lx. Data are presented as mean ± SD (n = 5); ***P < 0.001, **P < 0.01, *P < 0.05, marked necessarily.

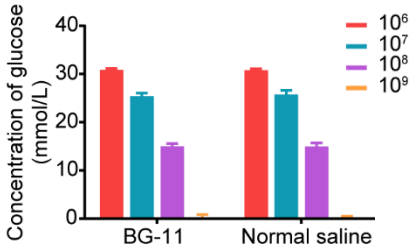

Figure S6 Glucose remaining in the BG-11 medium (with 33 mmol/L glucose) with/without nitrogen supplement after 12 h incubation, 37 °C, 800 lx. The concentrations of Chlorella were 1×10^6, 1×10^7, 1×10^8 and 1×10^9 cell/mL. Data are presented as mean ± SD (n = 6).

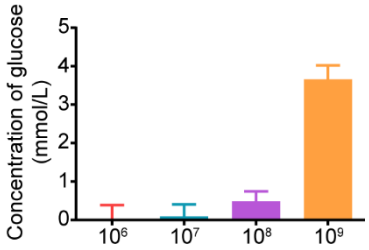

Figure S7 The inherent glucose of Chlorella. The concentrations of Chlorella were 1×10^6, 1×10^7, 1×10^8 and 1×10^9 cell/mL. Data are presented as mean ± SD (n = 6).

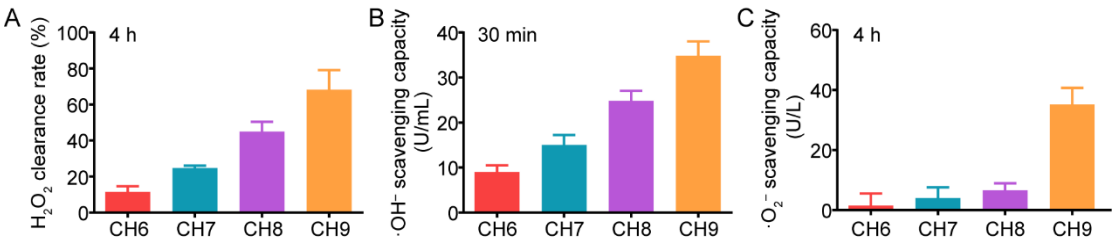

Figure S8 (A) The depletion of H_2O_2 and (B, C) the inhibition of $·OH^-/·O_2^-$ generation by Chlorella hydrogels in transwell, 37 °C, dark, respectively. Data are presented as mean ± SD (n = 6).

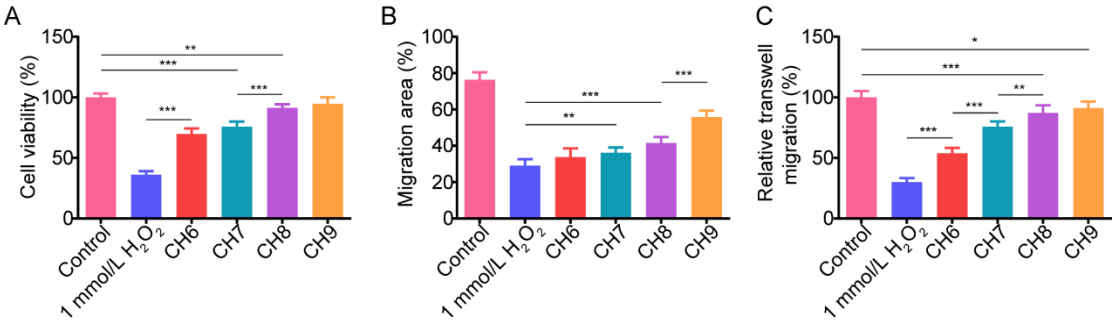

Figure S9 Quantitative analysis of (A) L-929 cell proliferation, (B) HaCaT migration and (C) transwell migration of HUVEC by ImageJ software, 37 °C, dark. The concentration of H_2O_2 in the cell culture medium was 1 mmol/L. Data are presented as mean ± SD (n = 5); ***P < 0.001, **P < 0.01, *P < 0.05, marked necessarily.

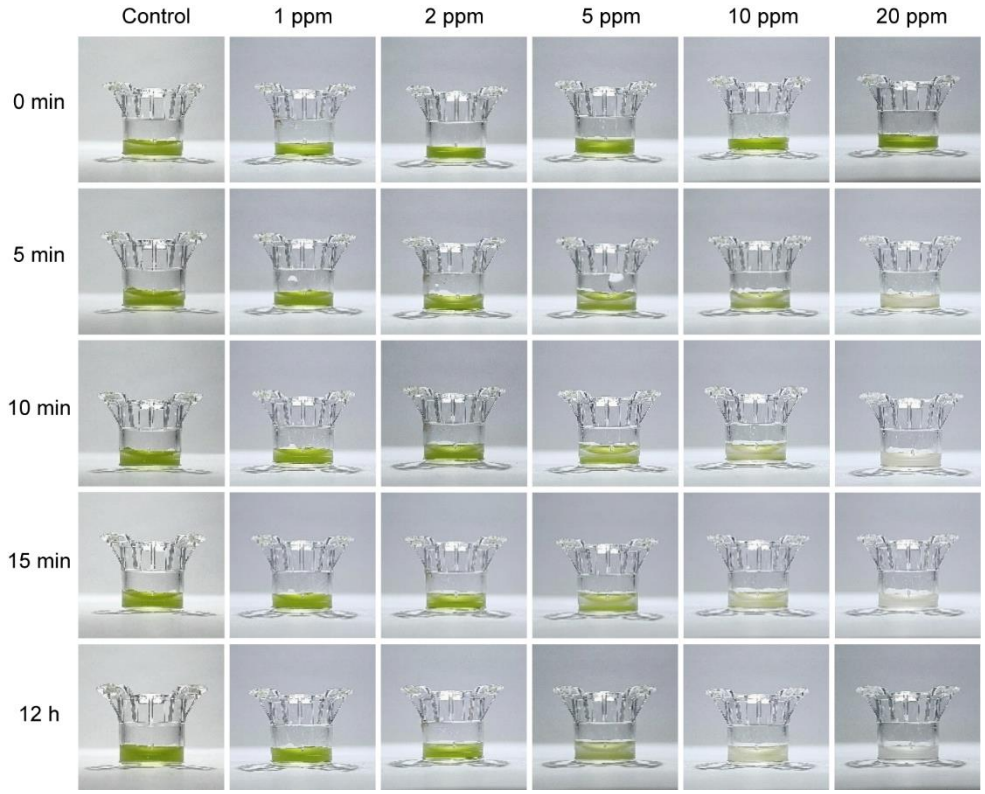

Figure S10 Photographs of Chlorella hydrogels inactivated by chlorine dioxide. Chlorella concentration: 1×10^8 cell/mL.

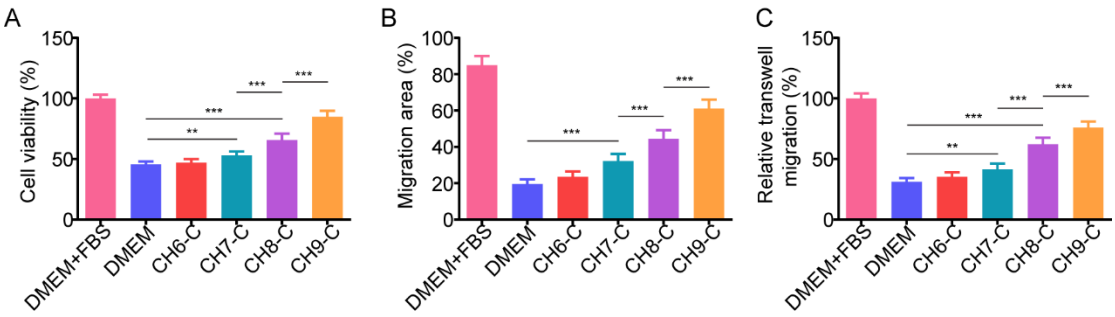

Figure S11 Quantitative analysis of (A) L-929 cell proliferation, (B) HaCaT migration and (C) transwell migration of HUVEC by ImageJ software, 37 °C, dark,. Basic DMEM was selected as the cell culture medium. Data are presented as mean ± SD (n = 5); ***P < 0.001, **P < 0.01, *P < 0.05, marked necessarily.

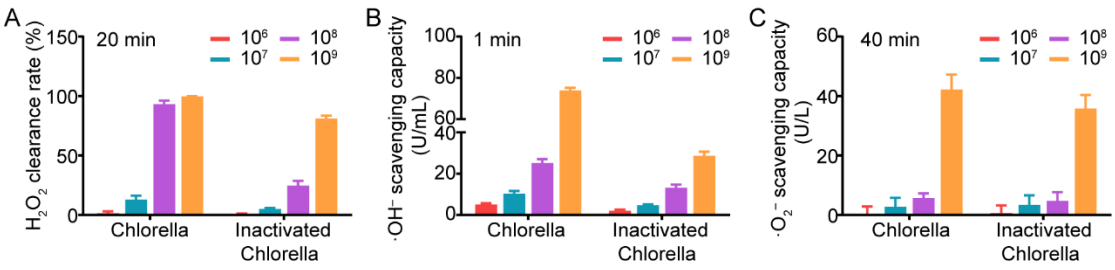

Figure S12 The comparison of Chlorella and inactivated-Chlorella on the depletion of (A) H_2O_2 and (B, C) the inhibition of $·OH^-$/$·O_2^-$ generation in BG-11 medium, respectively. The concentration of Chlorella was 1×10^6, 1×10^7, 1×10^8 and 1×10^9 cell/mL. Data are presented as mean ± SD (n = 6).

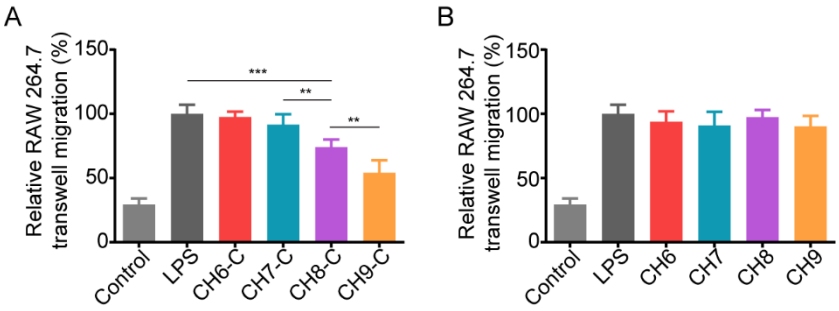

Figure S13 Quantitative analysis of the effect of (A) inactivated-Chlorella hydrogels and (B) Chlorella hydrogels on RAW 264.7 cell transwell migration by ImageJ software. Data are presented as mean ± SD (n = 5); ***P < 0.001, **P < 0.01, *P < 0.05, marked necessarily.

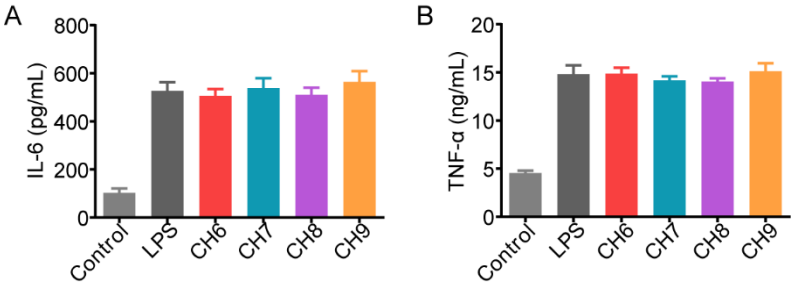

Figure S14 The secretion of (A) IL-6 and (B) TNF-α by LPS-induced RAW 264.7 cells treated with Chlorella hydrogels. Data are presented as mean ± SD(n = 6).

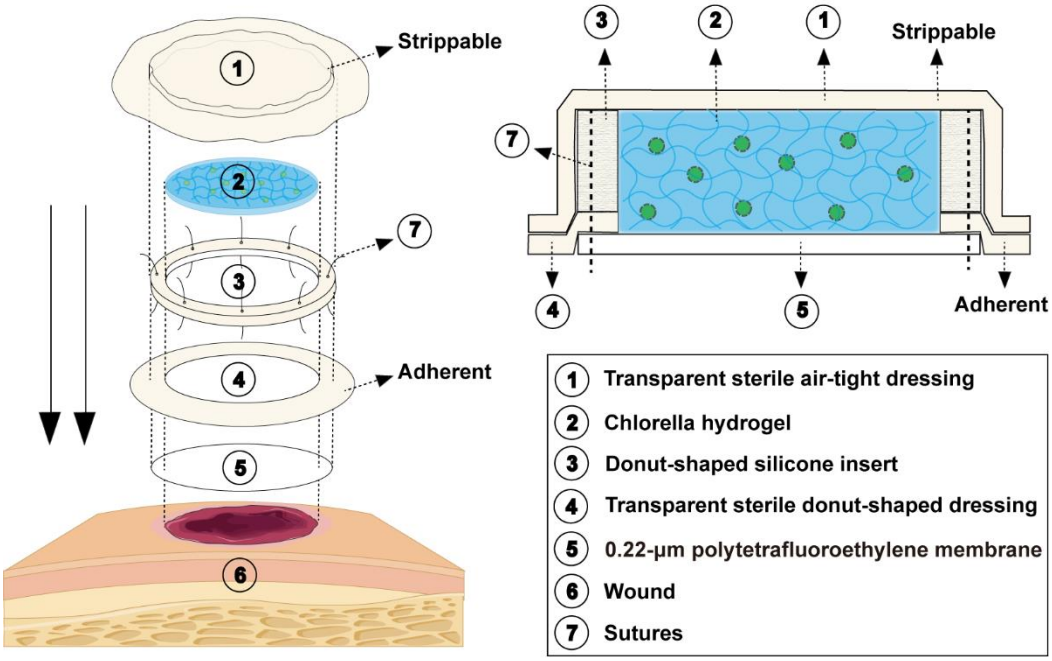

Figure S15 Schematic diagram of the application of Chlorella hydrogels in the *in vivo* wound healing experiment. A transparent sterile air-tight dressing was used to reduce the leakage of oxygen. 0.22-μm polytetrafluoroethylene membrane was used to avoid the diffusion of Chlorella into the wound tissue. In the CH8-C group, the transparent sterile air-tight dressing was opened after 12 h illumination and the chlorine dioxide was secondary delivery, then the dressing was stuck again. Transparent sterile air-tight dressing and Chlorella hydrogels were renewed daily for all the groups.

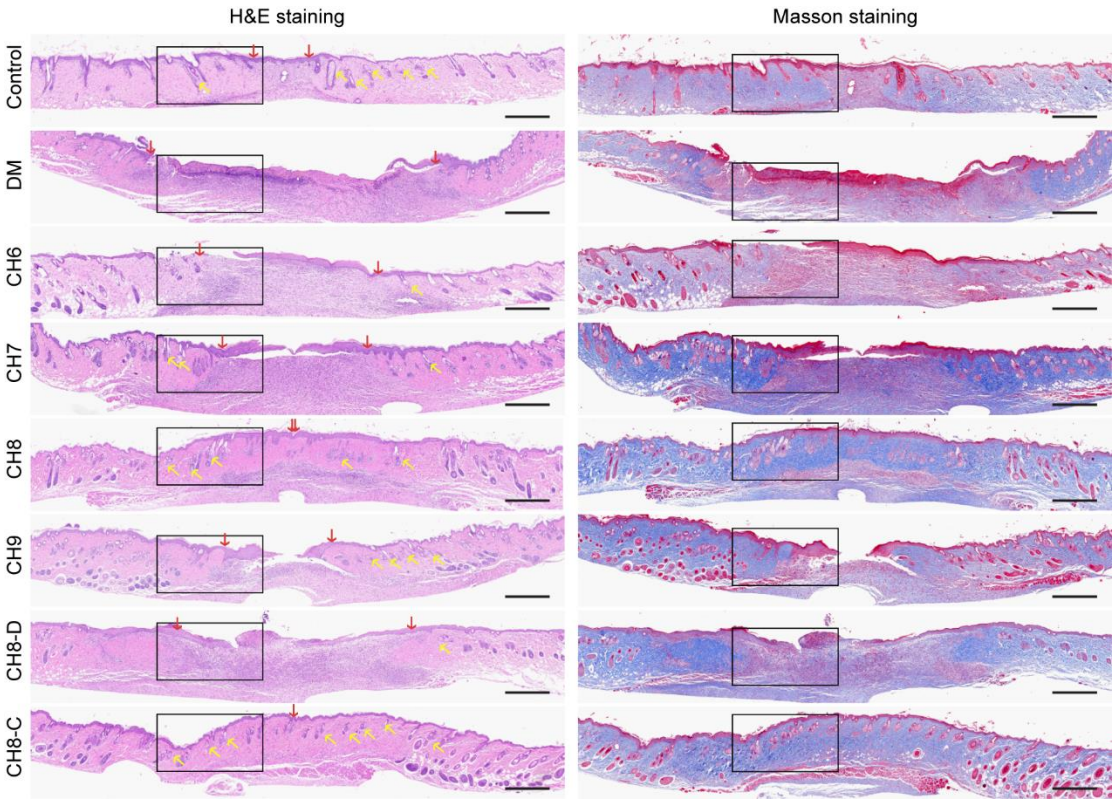

Figure S16 Photographs of H&E staining and Masson staining. Black frame, the selected area in Fig. 7C and G; red arrow, granulation tissue gap; yellow arrow, hair follicle. Scar bar: 500 μm.

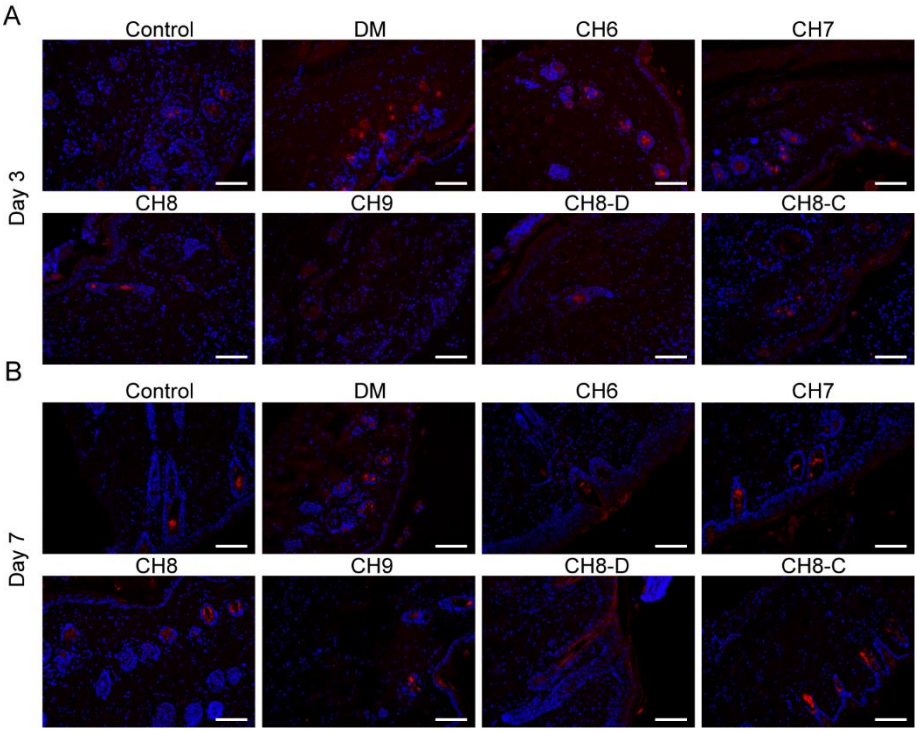

Figure S17 Representative images of immunofluorescence staining of IL-6 (red) in the wound tissue on (A) Day 3 and (B) Day 7 after wounding. Scale bar: 100 μm.

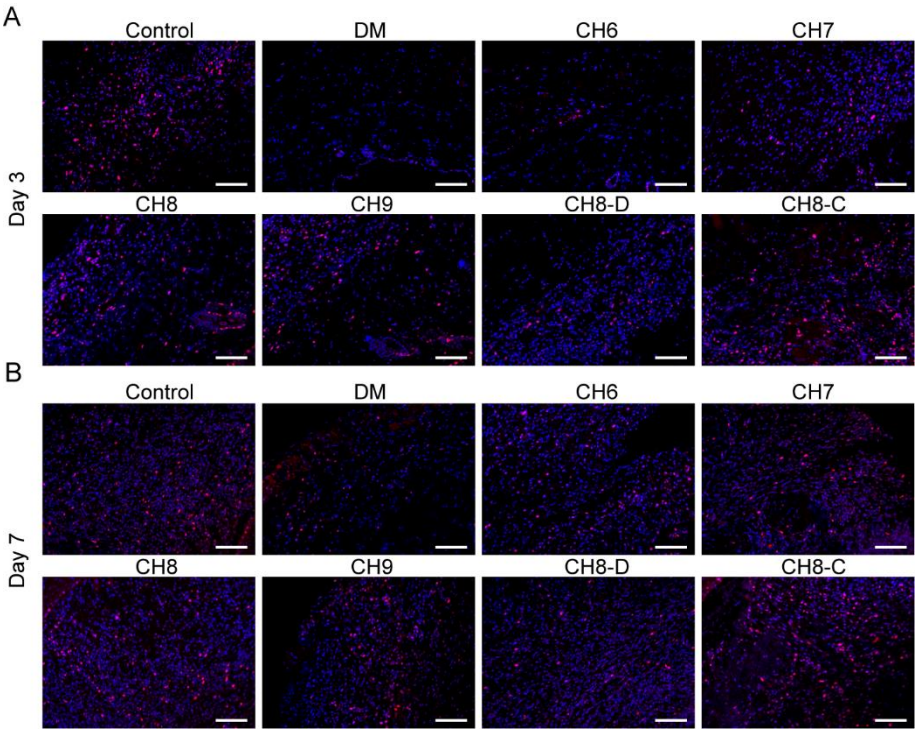

Figure S18 Representative images of immunofluorescence staining of Ki67 (red) in the wound tissue on (A) Day 3 and (B) Day 7 after wounding. Scale bar: 100 μm.

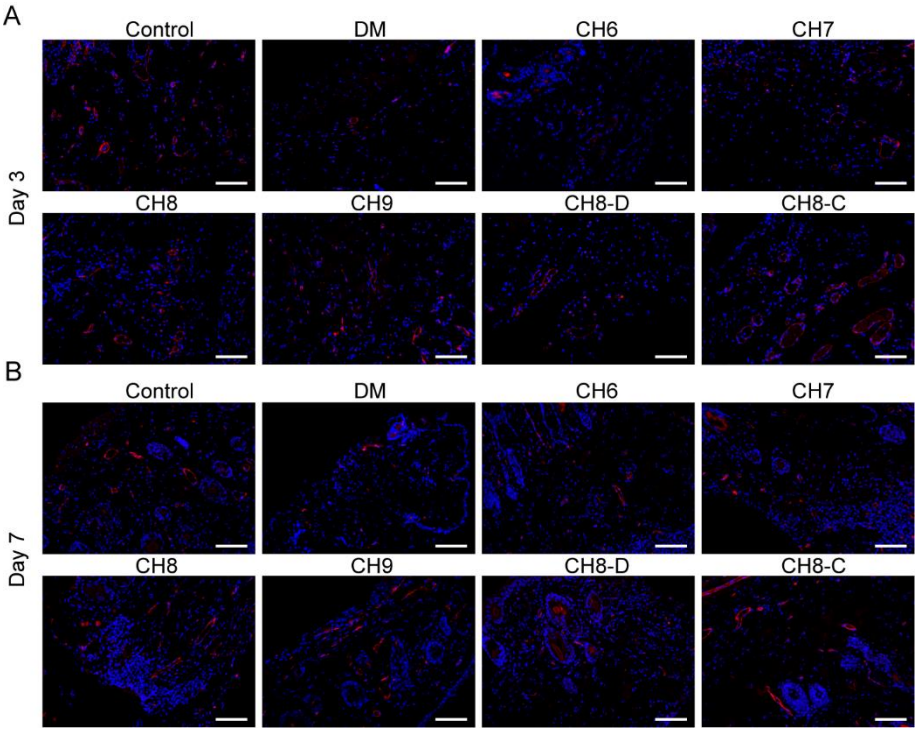

Figure S19 Representative images of immunofluorescence staining of VEGF (red) in the wound tissue on (A) Day 3 and (B) Day 7 after wounding. Scale bar: 100 μm.

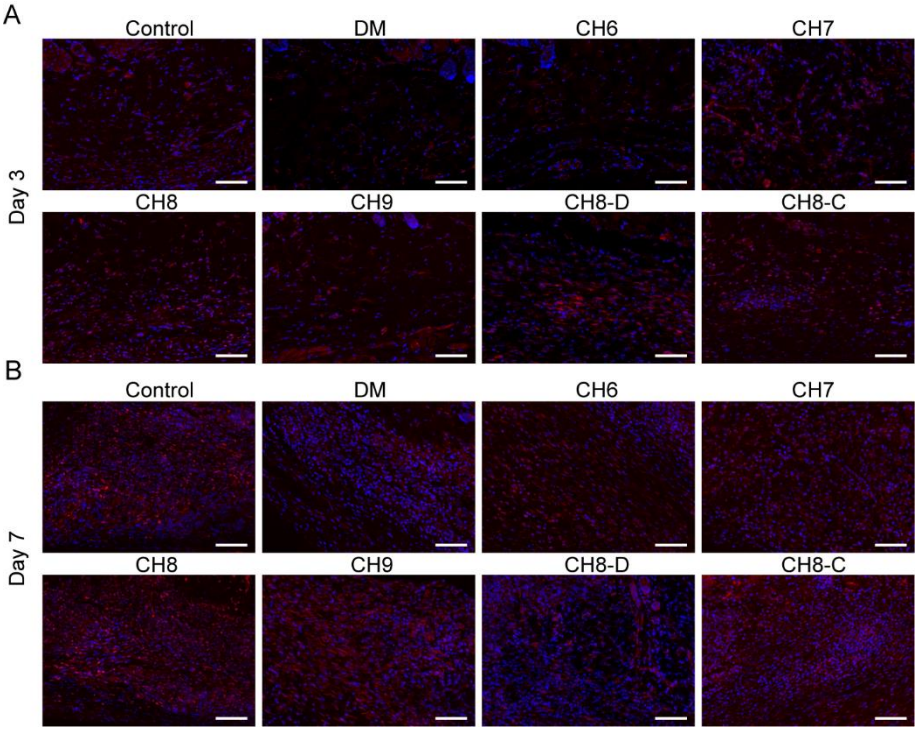

Figure S20 Representative images of immunofluorescence staining of CD31 (red) in the wound tissue on (A) Day 3 and (B) Day 7 after wounding. Scale bar: 100 μm.